Low-energy electron microscopy study of step mobilities on Si(001)

N. C. Bartelt*
Department of Physics, University of Maryland, College Park, Maryland 20742

R. M. Tromp
IBM Research Division, Thomas J. Watson Research Center, P.O. Box 218, Yorktown Heights, New York 10598

(Received 28 May 1996)

We have analyzed low-energy electron microscopy observations of the equilibrium fluctuations of steps on Si(001) in the temperature range 640–1170 °C. By examining the wavelength dependence of the time constants of the fluctuations, we find that the step motion is limited by the rate of random attachment and detachment of adatoms at the step edges. From the values of the time constants, we determine the step mobility which in principle governs how fast a step responds to being out of equilibrium. This mobility is the same, within experimental uncertainty, for S_A and S_B steps. By studying the decay of nonequilibrium rough step profiles, we explicitly show that the step motion is curvature driven, and that the mobility deduced from the thermal fluctuations quantitatively accounts for step smoothing rates. From the amplitude of the equilibrium fluctuations, we determine the stiffnesses of the S_A and S_B steps as a function of temperature. [S0163-1829(96)05540-3]

I. INTRODUCTION

Given enough surface mobility, the arrangement of steps on a surface is governed by well-understood principles of equilibrium surface statistical mechanics. However, the mobility of steps, which governs the equilibration of step structure and surface morphology, is in general not well quantified. The large-scale motion of steps needed to change surface morphology is determined by a very large number of atomic events. The problem is to determine how statistical correlations between atomic events collaborate to cause large-scale fluctuations in the step-edge positions. Some recent work, most notably with scanning tunneling microscopy (STM), has been able to characterize the atomic mechanisms of step motion. For example, Kuipers *et al.*[1] find that steps on Au(110) move by random attachment of atoms at kink sites, while Giesen-Seibert *et al.*[2] find that steps on Cu(1 1 19) fluctuate predominantly by atoms hopping along step edges.

In this paper we use low-energy electron microscopy (LEEM) to study the thermal fluctuations of step edges on vicinal Si(001) on a larger length scale than the STM studies. This more macroscopic approach has some advantages. Even if the individual atomic processes at step edges can be characterized, it is still not obvious which processes are important for large-scale changes in surface morphology. By observing large-scale equilibrium thermal fluctuations, however, we can quantify the diffusion coefficients governing macroscopic step motion. Second, in LEEM the temperature dependence of these step mobilities can be probed over a wide range, allowing activation energies to be determined. Here we were able to study fluctuations from 640 to 1170°C. Third, a huge amount of data can be readily collected and analyzed, allowing the correlation functions needed to quantify step energetics and dynamics to be accurately measured.

The behavior of steps on Si(001) has been the subject of a large number of studies. For small miscut angles, the equilibrium step structure consists of alternating single-layer height S_A and S_B steps, interacting through long-ranged elastic strain fields. Previous STM work[3–6] on step dynamics for Si(001) below 450 °C has established that, at low temperature, changes in step position occur in units of pairs of dimers, although the nature of the events leading up to the changes is unknown. There is some evidence that the events are correlated along the step edge.[4]

Our basic approach (following Refs. 7 and 8) in analyzing the step fluctuations is to study the dependence of the amplitudes and time constants of the fluctuations as a function of their wavelength and temperature. As reviewed in Sec. II, the amplitude of the thermal fluctuations determines the step-edge stiffness, while the time constant allows the nature of the kinetic processes determining the step-edge mobility to be determined and quantified. Using this mobility we can make and check predictions about how step structures which are out of equilibrium will relax. We do this in two ways. First, we show that the mobilities which we extract from the step fluctuations quantitatively account for how a step edge which is roughened by depositing atoms at low temperature smooths when heated. Second, we find that the relaxation times observed by Webb *et al.*[9] for stress-induced pairing of S_A and S_B steps compares favorably with the times predicted from our measured step mobilities. Other successful applications of these measured step mobilities on Si(001) are to observations of the dissolution of isolated islands, as well as to the Ostwald ripening of a family of islands. Those results are discussed elsewhere.[10,11]

A brief discussion of some of the results presented in this paper appears in Ref. 12. There it was found that the increasing amplitude of the step fluctuations as a function of temperature eventually leads to an equilibrium roughening phase transition on Si(001) at around 1200 °C. Here we focus more on the dynamic, as opposed to equilibrium, aspects of the steps.

II. STEP FLUCTUATION THEORY

Let $x(y,t)$ be the position of the step edge as a function of the distance y along the step edge and the time t. We define the Fourier component x_q of the step edge by

$$x(y,t)=\sum_q x_q(t)\exp(iqy). \tag{2.1}$$

We study the fluctuations in the step edge by examining the correlation function $G_q(t-t')$ for each Fourier component:

$$G_q(t-t')=\langle |x_q(t)-x_q(t')|^2\rangle. \tag{2.2}$$

For wavelengths larger than a few lattice constants, this correlation function is expected to have the general form[8,13]

$$G_q(t)=A(q)[1-\exp(-|t|/\tau(q))]. \tag{2.3}$$

For an isolated step, the amplitude $A(q)$ of the fluctuations is determined by the step-edge stiffness $\tilde{\beta}$:

$$A(q)=\frac{2kT}{L\tilde{\beta}q^2}, \tag{2.4}$$

where L is the (analyzed) length of the step. (This equation can be simply thought of as a consequence of equipartition of energy among the modes of the ''vibrating'' step.[14]) The step-edge stiffness is a measure of the free-energy cost of bending a step edge.[14] If $\beta(\theta)$ is the step free energy per unit length as a function of the step orientation angle θ, the stiffness $\tilde{\beta}$ is defined as

$$\tilde{\beta}=\beta+\frac{\partial^2\beta}{\partial\theta^2}. \tag{2.5}$$

The step-edge stiffness is a thermodynamic quantity determined by the energy required to create atomic kinks in the steps. If one assumes that kink excitations are uncorrelated along the step edge [as has been established for Si(001) from STM studies[15]], then

$$\tilde{\beta}=kTa/b^2, \tag{2.6}$$

where a is the lattice constant, b^2 is the mean-square size of each kink site,

$$b^2(T)=\frac{\sum_n a^2n^2\exp(-E(n)/kT)}{\sum_n \exp(-E(n)/kT)}, \tag{2.7}$$

and $E(n)$ is the energy of a kink of length na. From STM studies of the kink structure, Swartzentruber *et al.*[15] proposed that

$$E(n)=n\epsilon+C, \tag{2.8}$$

where ϵ is the kink energy, estimated to be 28 ± 2 meV/atom for the S_B step edge and 90 ± 10 meV/atom for the S_A step, while the corner energy C is estimated to be 80 ± 20 meV. We will compare the temperature dependence of the stiffness predicted by this kink Hamiltonian with LEEM observations in Sec. VI.

The time constant of the step fluctuations [$\tau(q)$ in Eq. (2.3)] will increase as the wavelength of the fluctuations becomes larger, because large-wavelength fluctuations require more mass transport to occur. The exact dependence of the time constant on wavelength is determined by the microscopic kinetics. Perhaps the simplest possibility [and one which we will show appears to apply to Si(001)], is when attachment and detachment of atoms from the step edge is the rate-limiting step for step motion. In this case, any point on a curved step edge will relax at a rate proportional to the (mean) curvature at that point,[16,17] i.e.,

$$\frac{\partial x}{\partial t}=\frac{\tilde{\beta}\Gamma}{kT}\frac{d^2x}{dy^2}, \tag{2.9}$$

where Γ is the step mobility. This leads to a time constant proportional to the inverse square of the wave number,[8]

$$\tau(q)=\frac{kT}{\Gamma\tilde{\beta}q^2}. \tag{2.10}$$

A basic assumption of the Langevin approach used here and in Refs. 7 and 8 to study thermal fluctuations of steps is that the same time constants which govern thermal fluctuations also determine the relaxations of a system which is slightly out of equilibrium. This relationship will be tested explicitly in Sec. VII below. If the noise of attachments and detachments is completely random in units of the area occupied by an adatom ω, then the mobility Γ has the microscopic interpretation of[7]

$$\Gamma=\frac{\omega^{3/2}}{\tau_a}, \tag{2.11}$$

with τ_a^{-1} the attachment or detachment rate of adatoms averaged along the step edge.

Equation (2.10) represents the simple situation in which diffusion on the terraces and diffusion along the step edges are fast compared to the rate of exchange between the step edge and the adatom sea on the terraces. In the general case, when all three processes are acting simultaneously, the time constant for step-edge decay can be shown to be[18]

$$\tau(q)=\frac{kT}{\Gamma\tilde{\beta}q^2}\left(\frac{\Gamma+2c_0D^t\omega^2q+\omega^{3/2}D^sq^2}{2c_0D^t\omega^2q+\omega^{3/2}D^sq^2}\right), \tag{2.12}$$

where D^t is the diffusion coefficient for adatoms on the terraces, c_0 is the equilibrium adatom concentration on the terraces, and D^s is the diffusion coefficient for atoms along the step edge. When D^s and D^t (or q) are sufficiently large, one recovers Eq. (2.10). In the limit where Γ is very large and D^s (or q) is small, step fluctuations are limited by diffusion on the terraces, and one has[13,19]

$$\tau(q)=\frac{kT}{2D^tc_0\omega^2\tilde{\beta}q^3}. \tag{2.13}$$

On the other hand, if Γ is large and D^t is sufficiently small, step fluctuations will be limited by diffusion along the step edge,[7] and

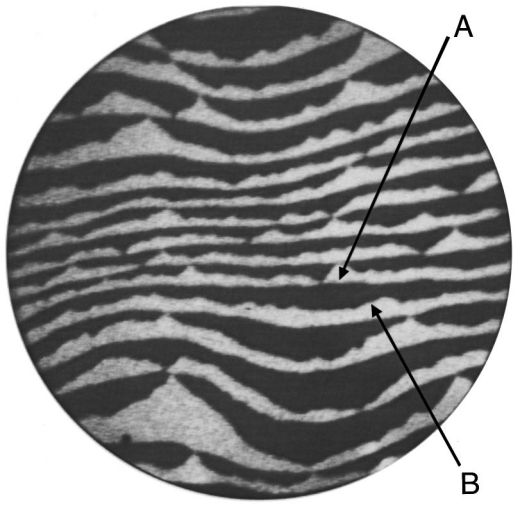

FIG. 1. LEEM image of Si(001) at 860 °C. The field of view is 4 μm. The step up direction points upwards on the figure. The two types of steps, S_A and S_B, are labeled A and B. The fluctuations of these labeled steps was studied from 640 to 1170 °C.

$$\tau(q)=\frac{kT}{D^s\tilde{\beta}\omega^{3/2}q^4}. \tag{2.14}$$

Since the wave-number dependence of the time constant is different for each mechanism, by measuring $\tau(q)$, LEEM data can be used to distinguish these different models, as we show below.

III. LOW-ENERGY ELECTRON MICROSCOPY DATA

The low-energy electron microscope used in these studies is described in Ref. 20. The Si(001) surface was cleaned by flashing to 1200 °C several times. A sample LEEM image of the studied region is shown in Fig. 1. It was formed by using the $(\frac{1}{2},0)$ LEED beam at $\approx$3.5-eV energy. The terraces alternate from black to white because of the 90° rotation of the (2×1) reconstruction across the single-atomic-layer height steps. The average terrace width in the studied region was 130 nm (which corresponds to a 0.04 degree miscut).

Crystals were heated by electron bombardment from the rear. The temperature was measured using an optical pyrometer. Video sequences of the surface (4-μm field of view) were recorded at 640, 713, 790, 860, 920, 977, 1028, 1100, and 1170 °C. The analyzed sequences typically lasted 2 min (slightly less at higher T). The temperature was stable to 10°C during this time. The sample drift was small enough that the same step edges formed part of all the analysis presented here. (For example, the step edges labeled A and B in Fig. 1 were analyzed at all temperatures.)

At all the temperatures studied, the S_A and S_B steps were observed to fluctuate independently of each other: there was no intrinsic tendency to double as is sometimes reported at high temperature. Overall step motion due to sublimation[21] was always much slower than the studied fluctuations. There was no indication that sublimation strongly affected step structure as it (dramatically) does on high-temperature vicinal Si(111).[22]

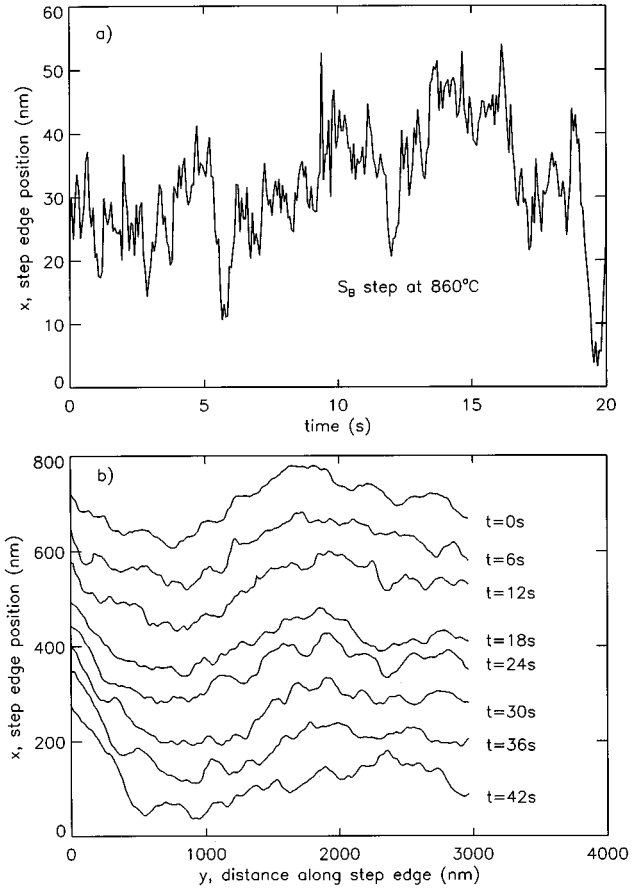

FIG. 2. (a) The fluctuations in time of one particular point on the step edge at 860 °C. (b) The time dependence of a marked S_B step, at 977 °C. (For clarity, the average position of the step has been offset at each time.)

An advantage of the Fourier-transform technique of analyzing step fluctuations is that effects due to the inevitable drift of the sample in the microscope are largely felt only by the $q=0$ component of the Fourier transform, which we have not attempted to analyze here.

IV. ANALYSIS PROCEDURE

The video frame rate is 30 per second. We captured and analyzed all of these frames at 640×480 resolution: each pixel corresponds to 8.5 nm. To aid the fitting procedure the data were smoothed by taking a square boxcar average of area nine pixels. As discussed in more detail below, fluctuations in image intensity usually made some time averaging necessary.

The step-edge positions were determined by least-squares fitting the image intensity to a hyperbolic tangent with a width of one pixel in a direction perpendicular to the average step direction. The fits used the image intensity of the 50 nm on either side of the step edge. The two types of steps were distinguished by fixing the sign of the hyperbolic tangent to be positive or negative. (This avoids the confusion that can be caused by S_A and S_B steps getting near to each other.) The length of the marked steps ranged from 1 to 3 μm. Because of flaws in a small percentage ($\sim$3%) of the images (caused, for example, by the image intensity momentarily decreas-

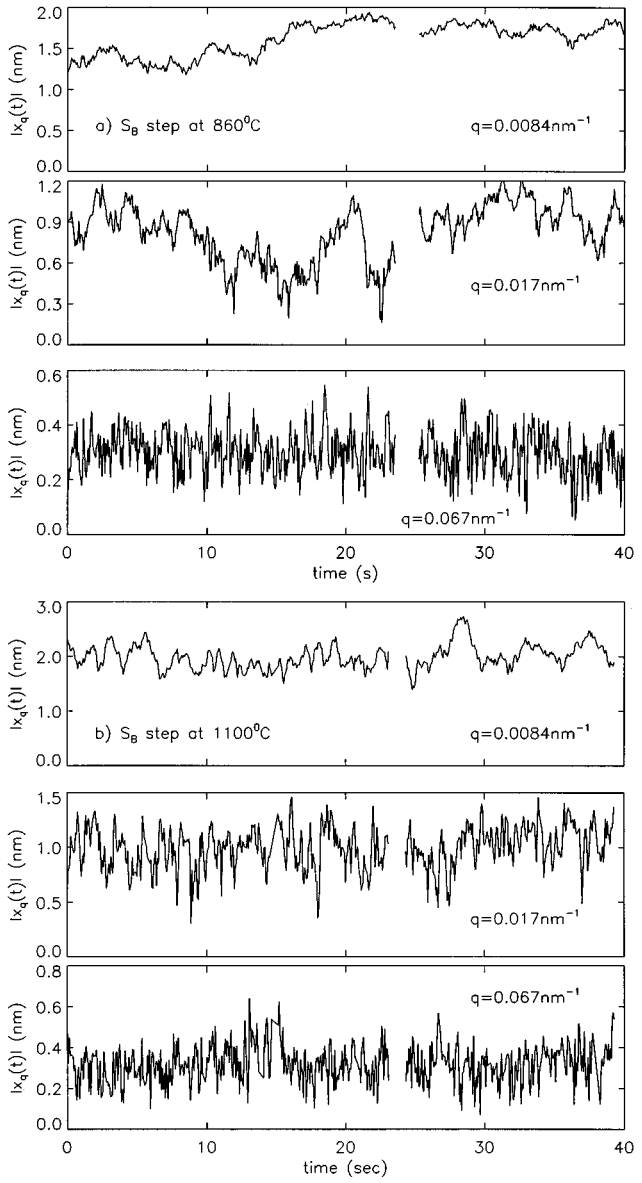

FIG. 3. The time dependence of several Fourier components of a step of length $L=3\mu$m. The components shown are for an S_B step at (a) 860 °C and (b) 1100 °C.

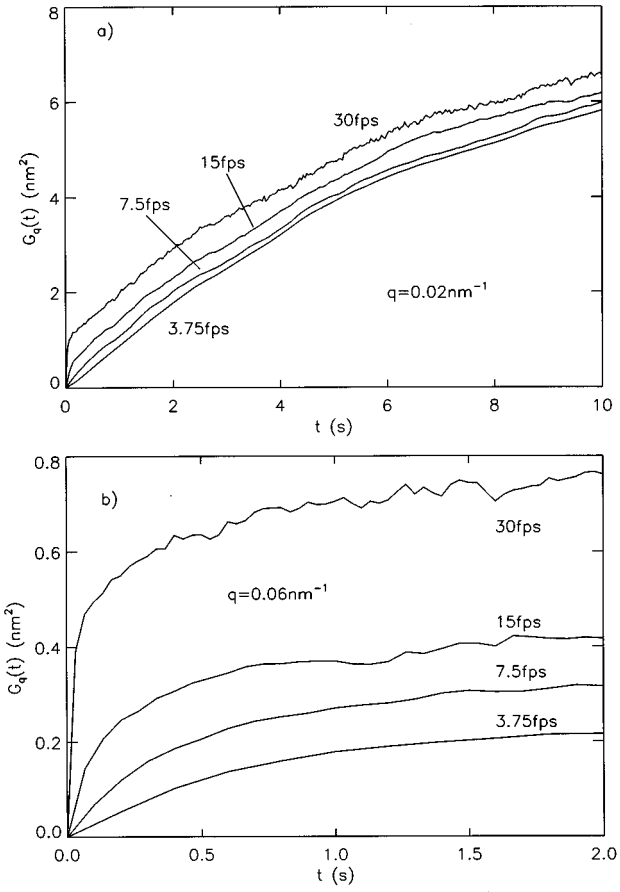

FIG. 4. Time correlation functions for a 3.0-μm length of a S_B step at 790 °C. The four curves in each figure from top to bottom show the results of no time averaging, averaging over two video frames, four frames, and eight frames, respectively. Panel (a) shows $G_q(t)$ for $q=0.02$ nm^{-1} (wavelength approximately 300 nm). Panel (b) shows $G_q(t)$ for $q=0.06$ nm^{-1} (wavelength approximately 100 nm).

ing), some steps in the video sequences could not be fit, and were dropped from the analysis. To give an idea of the scale of the fluctuations in step position, Fig. 2(a) shows the time dependence of one position along the step edge at 860°; Fig. 2(b) shows the fluctuations of the entire step edge at 977 °C.

To obtain the Fourier components x_q of Eq. (2.1), spurious small-wavelength effects due to the fluctuations at the ends of the marked step edge were minimized by multiplying the data by a window function[23]

$$w(y)=1-\left(\frac{2y-L}{L}\right)^2, \tag{4.1}$$

where the step ends are at $y=0$ and $y=L$.

Figure 3(a) shows the time dependence of the three different Fourier components for a S_B step edge at 860 °C. As expected, the larger the wavelength, the larger the time scale of the fluctuations. Figure 3(b) shows the same for step at 1100 °C. For the same wavelength, the time scale of the fluctuations is much faster — and the amplitude is slightly larger.

Because of random fluctuations in the image intensity, random errors on the order of the pixel size are made in the fitting process. These uncertainties lead to short-time-scale fluctuations of even the very large-wavelength components shown in Fig. 3. The effect of this random noise on the measured step correlations is easily detected by varying the frame averaging rate. Figure 4 shows the variation in $G_q(t)$ for one particular wavelength at 790 °C. At 30 frames per second the noise in marking the step edge is evident from the large jump at small t: the many-second time scale is due to real fluctuations of the step edge, while the very short-time-scale fluctuations are due to step marking uncertainties. As shown in the figure, marking steps after averaging the image intensity over (successively) two, four, and eight frames largely removes this random component, without distorting the form of the correlation functions. On the other hand, when the wavelength is small and the fluctuations are on the order of the video rate, averaging has serious detrimental

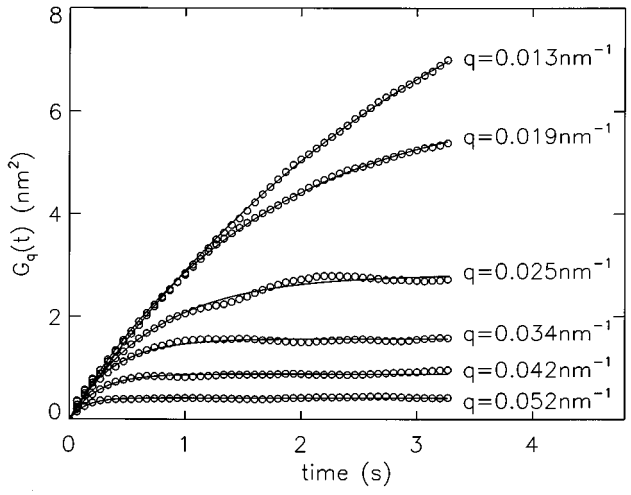

FIG. 5. The dependence of $G_q(t)$ on wavelength for an S_B step at 860 °C. As q increases, both the time constant and amplitude of the fluctuations decrease. The solid lines shows the fits to Eq. (2.3) from which $A(q)$ and $\tau(q)$ were extracted.

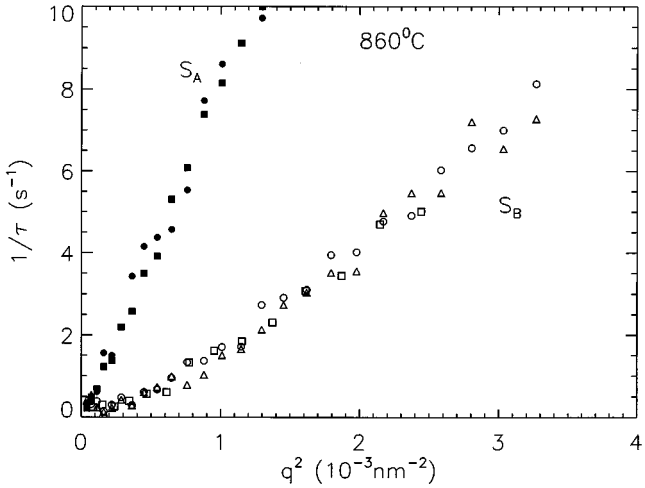

FIG. 6. The q dependence of the fitted time constant for several S_A and S_B steps at 860 °C. Each symbol corresponds to a different step.

effects: it tends to diminish the magnitude of the fluctuations, as seen in Fig 4(b). Above 800 °C, averaging over two frames provided a good compromise. Below this temperature, however, averaging over four or eight frames becomes necessary to reduce noise effects, especially for the small amplitude S_A fluctuations.

Instrumental resolution will also tend to decrease the amplitude of the measured fluctuations as small wavelengths. The finite resolution of the instrument can, at least crudely, be corrected for. Suppose the marked step edge $x_m(y)$ is the convolution of a Gaussian with the actual step edge $x(y)$,

$$x_m(y) \propto \int_0^L x(y')\exp[-(y-y')^2/w^2]dy', \qquad (4.2)$$

where w measures the resolution to which we have marked the step edge. From the convolution theorem, this will cause the q dependence of $A(q)$ to change to $A(q)\exp(-w^2q^2/8)$. So dividing the measured $A(q)$'s by a Gaussian should allow us to estimate better the actual $A(q)$: the choice of the appropriate w will be briefly discussed below.

V. WAVELENGTH DEPENDENCE OF THE STEP FLUCTUATIONS: ANALYSIS AT 860 °C

The time dependence of the $G_q(t)$ for an S_B step at a temperature of 860 °C, determined by the method discussed in Sec. IV, is shown in Fig. 5. The exponential function of Eq. (2.2) fits experimental observations well. The increase in the time constant and amplitude with decreasing q is clearly visible. Figure 6 shows values of $\tau(q)^{-1}$ obtained from the exponential fits, for several different S_A and S_B steps, plotted as a function of q^2. As discussed in the Sec. II, the wavelength dependence of the time constant is determined by the nature of the rate-limiting atomistic process. The curves are to a good approximation linear for all of the steps, consistent with step-edge kinetics being attachment-detachment limited. There are several other notable features of these curves. First, the time constant for the S_A steps increases much more rapidly with q than the time constant for the S_B steps. Second, the time constants are roughly the same for all steps of the same type: they do not depend strongly on the local environment of the step edges. (For the three S_B steps

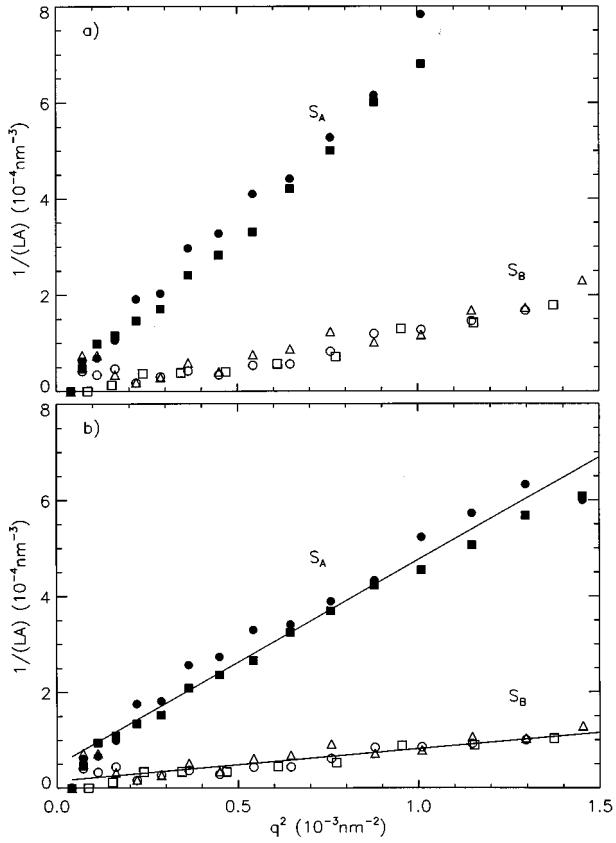

FIG. 7. (a) The amplitude of the fluctuations as a function of q^2 at 860 °C. (b) The same plot of the amplitude, corrected for the instrumental response by dividing by a Gaussian, with a width corresponding to a resolution of $\approx$50 nm. The slope of the lines gives the step-edge stiffness at this temperature of 0.13 and 0.88 kT/nm for the S_B and S_A steps, respectively.

shown, the distance to the nearest S_A step were approximately 100, 150, and 200 nm.)

Next we discuss the amplitude of the fluctuations, from which the step-edge stiffnesses can be extracted. Figure 7(a) plots the inverse of the amplitude of the fluctuations as a function of q^2. These plots are linear over much of the q range, as predicted by the equipartition of energy among the Fourier modes [Eq. (2.4)]. However, the inverse amplitudes at large q increase slightly faster than linear. This is probably not the effect of a small time constant smearing the fluctuations: Figure 6 shows that the time constants are still large compared to the frame capture rate. It seems reasonable that this is an effect of instrumental resolution. As shown in Fig. 7(b), a value of w can be chosen to make $1/A$ quadratic in q over the same range as the time constant is quadratic. This choice of w translates into a full width at half maximum of the original real-space Gaussian of 50 nm. This seems reasonable — the smoothing window used was about 25 nm and the resolution of the instrument is 15 nm. From Eq. (2.4) the slope[24] of the lines gives the step-edge stiffnesses $\tilde{\beta}$: at this temperature the stiffnesses are 0.13 and 0.9 kT/nm for the S_B and S_A steps, respectively. For comparison, the stiffnesses one deduces from Swartzentruber's kink Hamiltonian [Eq. (2.8)] using Eqs. (2.5) and (2.7) at this temperature are 0.08 and 1.45 kT/nm for the S_B and S_A steps, respectively. The significance of this comparison will be discussed in Sec. VI.

At extremely small q there is some tendency for the amplitude of the fluctuations to be larger than given by the q^2 dependence of Eq. (2.10). Perhaps this is due to the waviness of the steps caused by the desire for the surface to minimize the energy associated with the elastic strain fields associated with the steps.[25–27]

In previous studies of step capillary waves, the step mobility Γ has been estimated by using the stiffnesses deduced from $A(q)$ and fitting $\tau(q)$ to Eq. (2.10), using Γ as an adjustable parameter. This method relies on the time constants being short enough that the amplitude of capillary waves can be accurately determined. For most of the wavelengths studied this is clearly not a problem. However, for long, slowly varying wavelengths a better way of estimating Γ is to use the fact that the small t slope of $G_q(t)$, i.e., the relaxation rate of each Fourier component, can be estimated even if the amplitude is not fully equilibrated. The initial slope of $G_q(t)$ is $A(q)/\tau(q)$. From Eqs. (2.4) and (2.10) this ratio determines the step mobility in the case of attachment-detachment limited kinetics:

$$\Gamma = \frac{LA(q)}{2\tau(q)}. \tag{5.1}$$

Figure 8 plots this ratio at 860 °C for S_A and S_B steps. Consistent with the behavior of $\tau(q)$ and $A(q)$ individually, the ratio is indeed approximately constant. Remarkably, the mobility is roughly independent of whether the step is S_A or S_B. Thus the difference in the time constants for S_A and S_B steps shown in Fig. 6 can be attributed entirely to the differences in the step-edge stiffness. From this plot, we deduce a mobility of approximately 4×10^3 nm^3/s. From Eq. (2.11), using ω as the area of a dimer on Si(001),[28] this mobility corresponds to 2×10^4 exchanges of dimers with the terraces per dimer row per second.

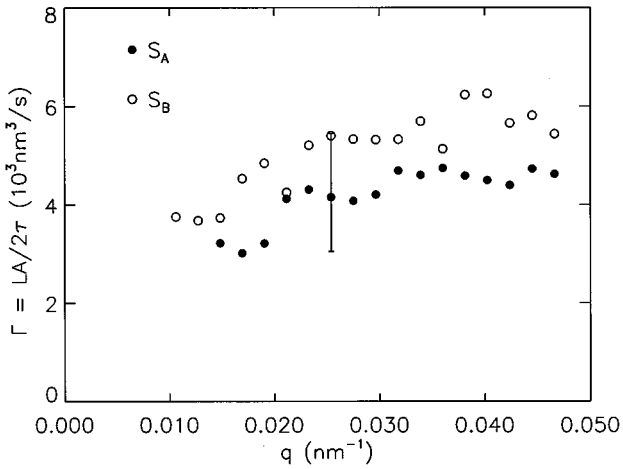

FIG. 8. The q dependence of the ratio of the amplitude to the time constant of the fluctuations at 860 °C determined from the small t slopes of $G_q(t)$ (Fig. 5). The closed circles are for an S_A step; the open circles are for an S_B step. If step kinetics is attachment-detachment limited, this ratio should be independent of q and equal to the step mobility Γ.

VI. TEMPERATURE DEPENDENCE

Following the same procedure as for the steps at 860 °C, we determined the step-edge mobility and stiffness from 640 to 1100 °C. Figure. 9 plots the ratio of the amplitude to time constant of Eq. (5.1) for the S_B steps for various temperatures. At all temperatures, the ratio does not depend strongly on q, consistent with attachment-limited step-edge kinetics. The mobility at each temperature was determined by averaging the ratio over the q ranges indicated in the figure. This range becomes smaller at high temperature because the increase in the mobility decreases the range over which the time constants of the fluctuations become small compared to the video rate. The high-q cutoffs at the higher temperatures correspond to time constants on the order of 0.1 s. As suggested by Fig. 8 at 860 °C, the plot for the S_A steps is within uncertainty the same at all temperatures. Figure 10 shows an

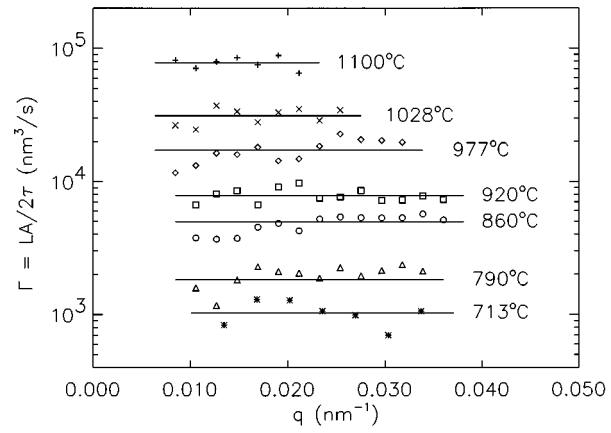

FIG. 9. The q dependence of the ratio of the amplitude to the time constant of step capillary waves for an S_B step at various temperatures. The step mobility Γ was estimated by averaging the ratio over the indicated ranges of q.

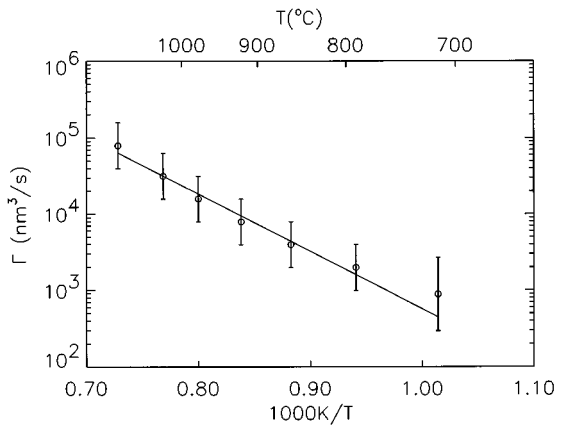

FIG. 10. An Arrhenius plot of the temperature dependence the ratio of amplitude to time constant for the S_B steps, showing the two-orders-of-magnitude rise in the step mobility. The corresponding plot for S_A steps is the same, within the estimated uncertainties.

Arrhenius plot of the step mobility from Fig. 9. The activation energy extracted from this plot is 1.45 ± 0.15 eV. Using Eq. (2.11), the rate of the exchange of dimers with the terraces ranges from 10^4 to 10^6 per second. Extrapolating the Arrhenius plots down to 475 °C yields a dimer exchange rate with the step edge of order one per second, consistent with STM observations.[3,6,4,5] The activation energy is consistent with the 1.3 ± 0.3 eV extracted from step-edge attachment rates observed at lower temperature by Swartzentruber and Schact[5] with STM, as well as the 1.4–1.7 eV range quoted by Kitamura *et al.*,[4] although significantly larger than the value 0.97 ± 0.12 reported by Pearson *et al.*[6] Approximately the same 1.45 eV activation energy was also obtained from analysis of island dissolution rates.[11]

Figure 11 shows the temperature dependence of the stiffnesses deduced from plots similar to Fig. 7. In contrast to the two order of magnitude change in the mobility over the studied temperature range, the stiffness of the S_B steps hardly

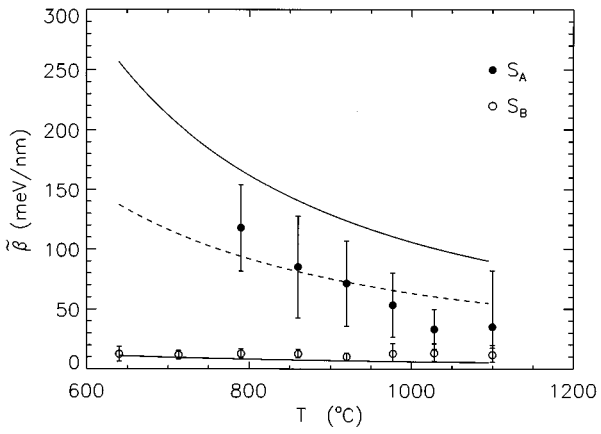

FIG. 11. The temperature dependence of the stiffnesses deduced from plots such as Fig. 7 (circles), compared with the predictions of Eqs. (2.5), (2.7), and (2.8) (solid line). Changing the S_A kink energy from 90 to 70 meV (dashed line) improves the agreement between theory and experiment.

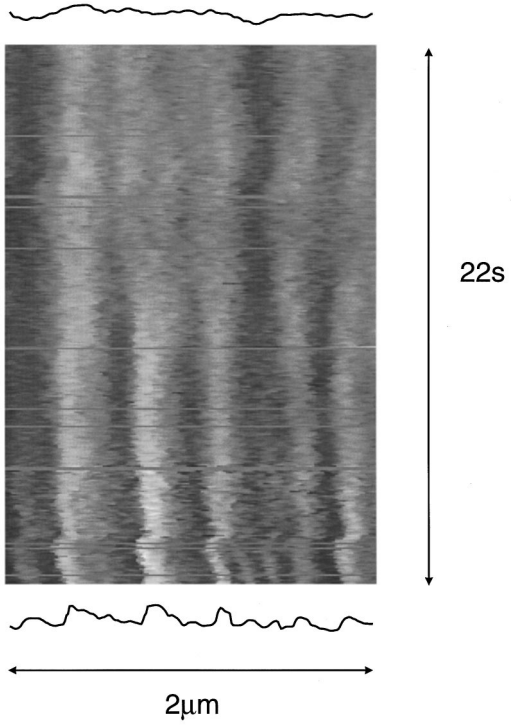

FIG. 12. A grayscale plot of the time dependence of the profile of a rough step at 800 °C. The bottom curve shows the rough starting step profile. The top curve shows the smoother step profile after 22 s.

changes at all, while the stiffness of the S_A steps only decreases by a factor of 3. Figure 11 also compares the capillary wave stiffnesses with the prediction of Swartzentruber's kink Hamiltonian using Eqs. (2.5), (2.7), and (2.8). The predicted S_A stiffness is always slightly too high. As discussed in Ref. 12 and shown by the dashed line, a kink energy of an S_A step of 70 rather than 90 meV yields better agreement with experiment. This change is within the experimental uncertainty of the S_A kink energy. The consequences of the observed temperature dependence of the stiffnesses is discussed in more detail in Ref. 12: the decrease in stiffness with increasing T eventually leads to a surface roughening temperature at around 1200 °C. At all temperatures, the ratio of step stiffnesses for the S_A and S_B steps derived from the capillary waves is in good agreement with observations of the equilibrium shape of two-dimensional islands.[12]

VII. EQUILIBRATION OF A ROUGH STEP EDGE

To test the prediction that the step mobility measured in the preceding sections actually governs the equilibration of step structure, we experimentally prepared a step which was much rougher than equilibrium, and monitored its smoothing to obtain equilibrium. To create the rough step, Si was deposited onto the surface at low temperature. The surface was then quickly heated to 800 °C. Figure 12 shows how the step profile relaxed during the next 22 s.

Figure 13 shows the time dependence of the square of four Fourier components of the step edge which had initial magnitudes much greater than expected from thermal fluctuations. The solid lines show fits to exponentials expected on the basis of Eq. (2.3). Figure 14 plots the inverse of the

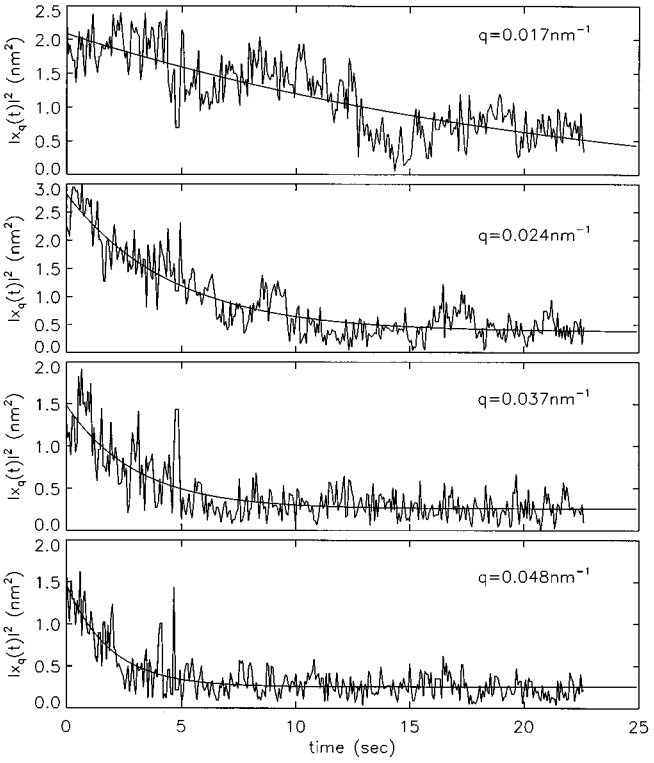

FIG. 13. The time dependence of four Fourier components of the step edge shown in Fig. 12. The smooth solid lines are fits to exponentials.

time constants extracted from these fits as a function of q^2. From Eq. (2.10), this plot should be linear with slope $\Gamma\tilde{\beta}/kT$. At 790 °C, from Figs. 9 and 11, $\tilde{\beta}$ and Γ are approximately 13 meV/nm, and 1800 nm^3/s, respectively. Thus one expects a value of $\Gamma\tilde{\beta}/kT$ of 260 nm^2/s. The best-fit slope of Fig. 14 is 245 nm^2/s. Given the uncertainties in all the fits, this agreement is surprisingly good. (For comparison the values of $\Gamma\tilde{\beta}/kT$ estimated from island dissolution rates in Ref. 11 are at least a factor of 2 lower than these capillary wave estimates.)

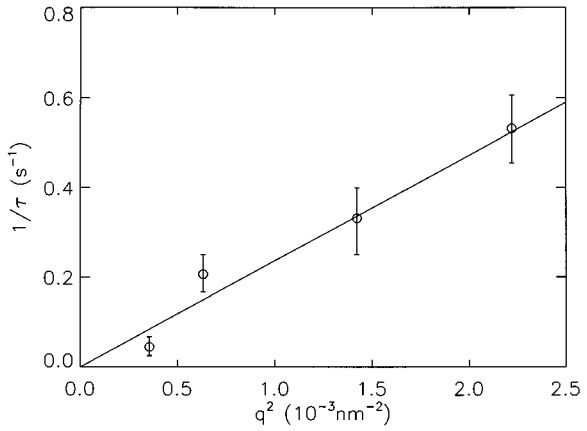

FIG. 14. The dependence on q^2 of the time constants extracted from the fits to exponentials shown in Fig. 13. The solid line is a least-squares fit. As discussed in the text, the slope of this line is consistent with that predicted from thermal step fluctuations.

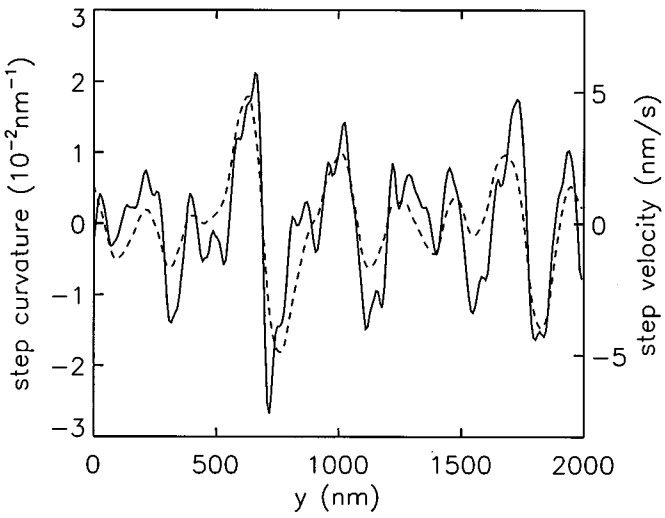

FIG. 15. A comparison of the velocity (dashed line) of the step edge shown in Fig. 12 with the average curvature (solid line). That the velocity is proportional to step curvature is direct evidence for adatom attachment-detachment kinetics. As discussed in the text, the proportionality constant is consistent with the step mobility extracted from thermal capillary wave analysis.

A more direct confirmation of the curvature-driven equilibration characteristic of attachment-detachment-limited kinetics is shown in Fig. 15. From the data shown in Fig. 12, we first extracted the average velocity of each point on the step edge, averaged over the middle 5 s of the sequence. We then determined the average curvature of each point along the step edge by taking the second derivative of the step profile averaged over the same 5 s. Figure 15 compares this curvature with the average velocity. They are clearly approximately proportional to each other. The best-fit ratio of step velocity to step curvature is 270 nm^2/s. Again from Eq. (2.9), the ratio should have the value $\Gamma\tilde{\beta}/kT$ which from the capillary wave analysis we estimated to be approximately 260 nm^2/s at 790 °C. The agreement is again better than one might expect, given the complexity of the analysis.

VIII. RELATIONSHIP WITH PREVIOUS OBSERVATIONS OF STEP MOTION

As mentioned in Sec. I, one reason that understanding step fluctuations is important is that they allow one to understand how an arrangement of steps (i.e., the surface morphology) which is out of equilibrium comes to equilibrium. One striking observation[9] of step equilibration is the relaxation of strain-induced step doubling on Si(001). We now try to relate this observation to our measurement of step fluctuations. First assume that the driving force for the step unpairing is the elastic repulsions between steps which is believed to have the form

$$E(l)=\lambda_\sigma \ln(l), \tag{8.1}$$

where E is the interaction energy per unit step length, l is the step separation and $\lambda_\sigma \approx 30$ meV/nm.[29,30] Next, we approximate the potential caused by the two neighboring steps by a quadratic potential with a minimum halfway between the

neighboring steps.[31] From Eq. (8.1), this approximation gives a potential $U(x)$ per unit length of the step edges of

$$U(x)=c(l)x^2=(\lambda_\sigma/l^2)x^2, \tag{8.2}$$

where x is the distance of the step from its average position between the two neighboring steps.

Since we believe that the step edges fluctuate and move by random attachment of adatoms or vacancies, then the equilibration time for exponential decay the average step-edge position to equilibrium is given by

$$\tau_{\rm eq}=kT/(2c(l)\Gamma)=kTl^2/(2\lambda_\sigma\Gamma), \tag{8.3}$$

where Γ is the step-edge mobility [see Eqs. (10) and (13) of Ref. 7].

If we extrapolate the Arrhenius plot of Γ in Fig. 10 down to 520 °C, then Γ is at most 20 $\rm nm^3/s$. This yields $\tau_{\rm eq}\approx 1000$ s. This compares with the 315 s reported by Webb *et al.*[9] for $l=150$ nm, with the value of l determined from the average sample miscut. Step waviness leads to a reduction in l by roughly $\sqrt{2}$, which modifies our estimate to $\tau_{\rm eq}=500$ s, reasonably close to the number of Webb *et al.* That these numbers are in rough agreement suggests that the mechanisms for step motion at lower temperatures might be the same as we observe at higher temperatures.

IX. CONCLUSIONS

By studying the thermal fluctuations of steps on Si(001) we have been able to determine the temperature dependence of the step mobilities which govern step equilibration. We have also shown that the numbers we obtain are consistent with observations of step relaxations.

From Figs. 10 and 11, the temperature dependence of the step fluctuations is marked by a very large decrease in the time scale of the fluctuations: while the stiffnesses change by at most a factor of 2 in the temperature range studied, the mobilities change by more than two orders of magnitude. The activation energy that we find for step attachment (1.45 eV) is much greater than kink creation energies ($\sim$ 0.1 eV). This observation suggests that changes in the step structure are not important for the observed changes in step mobility. It might have been natural, for example, to have supposed that atoms or vacancies are most likely to attach or detach at only particular kink sites, and that the number of these kink sites limit the fluctuations. This is what is observed to occur for steps on Au(110), for example.[1] There is evidence from STM measurements that this occurs on Si(001) at low temperature.[6] However, that the stiffnesses do not change much shows that the local step structure is not much affected by temperature, and does not play a crucial role in the temperature dependence of the step mobility. Further evidence supporting this picture is the fact that the adatom attachment rates for the S_A and S_B steps are comparable, despite their much different stiffnesses at low temperature.

Over the temperature range considered, the time constant of the fluctuations goes approximately like q^2, suggesting that fluctuations are due to *random* attachment and detachment of atoms at the step edges. This conclusion is consistent with the constant dissolution rate of epitaxially grown islands reported in Ref. 11. It is also consistent with step fluctuations observed at lower temperature with STM.[3] At the large wavelengths studied there is no evidence of the q^4 behavior characteristic of atomic diffusion along the step edges. It thus appears as if the correlations along the step edge detected by Kitamura *et al.*[4] do not strongly affect the large-scale motion of the step edges.

From Eq. (2.12), attachment-detachment-limited step relaxations only occur if $2c_0D^t\omega^2q\gg\Gamma$, i.e., if $\Gamma/\omega^{3/2}c_0D^t \ll 2\omega^{1/2}q$. Because c_0D^t is the hop rate of an adatom into a particular site on the terraces, and $\Gamma/\omega^{3/2}$ is the rate of hops onto the step edge from Eq. (2.11), $\Gamma/\omega^{3/2}c_0D^t$ is the probability s that an adatom incident on the step edge will become incorporated into it. From Figs. 8 and 9, it appears that a q-independent mobility, and thus attachment-limited kinetics, is seen for $q>0.01$ $\rm nm^{-1}$ at all studied temperatures. This implies that s is less than 0.01, assuming that dimers with $\omega=0.29$ $\rm nm^2$ are the primary diffusing species. One possible explanation for this low sticking probability is the low-temperature STM observation that changes in step-edge position always occur in units of pairs of dimers. Although it is completely unknown whether this persists to the high temperatures of this experiment, the structural changes needed to incorporate additional dimers into step edges seem likely to remain relatively complex, and thus slow, compared to dimer diffusion.

ACKNOWLEDGMENTS

We thank E. Williams for useful discussions, and Mark Reuter for his assistance with the experiments.

*Present address: Sandia National Laboratories, Livermore, CA 94551.

[1] L. Kuipers, M. S. Hoogeman, and J. W. M. Frenken, Phys. Rev. Lett. **71**, 3517 (1993); L. Kuipers, M. S. Hoogeman, J. W. M. Frenken, and H. van Beijeren, Phys. Rev. B **52**, 11 387 (1995).

[2] M. Giesen-Seibert, R. Jentjens, M. Poensgen, and H. Ibach, Phys. Rev. Lett. **71**, 3521 (1993); M. Giesen-Seibert, F. Schmitz, R. Jentjens, and H. Ibach, Surf. Sci. **329**, 47 (1995). See also L. Masson, L. Barbier, J. Cousty, and B. Salanon, *ibid.* **317**, L1115 (1994).

[3] H. J. W. Zandvliet, H. B. Elswijk, and E. J. van Loenen, Surf. Sci. **272**, 264 (1992); H. J. W. Zandvliet, B. Poelsema, and H. B. Elswijk, Phys. Rev. B **51**, 5465 (1995).

[4] N. Kitamura, B. S. Swartzentruber, M. G. Lagally, and M. B. Webb, Phys. Rev. B **48**, 5704 (1993).

[5] B. S. Swartzentruber and M. Schact, Surf. Sci. **322**, 83 (1995).

[6] C. Pearson, B. Borovsky, M. Krueger, R. Curtis, and E. Ganz, Phys. Rev. Lett. **74**, 2710 (1995).

[7] N. C. Bartelt, J. L. Goldberg, T. L. Einstein, and E. D. Williams, Surf. Sci. **273**, 252 (1992).

[8] N. C. Bartelt, J. L. Goldberg, T. L. Einstein, E. D. Williams, J. C. Heyraud, and J. J. Métois, Phys. Rev. B **48**, 15 453 (1993).

[9] M. B. Webb, F. K. Men, B. S. Swartzentruber, R. Kariotis, and M. G. Lagally, Surf. Sci. **242**, 23 (1991); M.B. Webb, *ibid.* **299/300**, 454 (1994).

[10] W. Theis, N. C. Bartelt, and R. M. Tromp, Phys. Rev. Lett. **75**, 3328 (1995).

[11] N. C. Bartelt, W. Theis, and R. M. Tromp, following paper, Phys. Rev. B **54**, 11 741 (1996).

[12] N. C. Bartelt, R. M. Tromp, and E. D. Williams, Phys. Rev. Lett. **73**, 1656 (1994).
[13] N. C. Bartelt, T. L. Einstein, and E. D. Williams, Surf. Sci. **312**, 411 (1994).
[14] P. Nozières in *Solids Far From Equilibrium*, edited by C. Godrèche (Cambridge University Press, Cambridge, 1991), p. 1.
[15] B. S. Swartzentruber, Y.-W. Mo, R. Kariotis, M. G. Lagally, and M. B. Webb, Phys. Rev. Lett. **65**, 1913 (1990).
[16] J. W. Cahn and J. E. Taylor, Acta Metall. **42**, 1045 (1994).
[17] For the thermal fluctuations studied here, the slope of the step with respect to the average orientation is always small, so that the step curvature accurately given by second derivative of the step position.
[18] H. P. Bonzel and W. W. Mullins, Surf. Sci. **350**, 285 (1996).
[19] A. Pimpinelli, J. Villain, D. E. Wolf, J. J. Métois, J. C. Heyraud, I. Elkinani, and G. Uimin, Surf. Sci. **295**, 143 (1993).
[20] R. M. Tromp and M. C. Reuter, Ultramicroscopy **50**, 171 (1993).
[21] J. J. Metois and D. E. Wolf, Surf. Sci. **298**, 71 (1993).
[22] A. V. Latyshev, H. Minoda, Y. Tanishiro, and K. Yagi, Phys. Rev. Lett. **76**, 94 (1996).
[23] W. H. Press, S. A. Teukolosky, W. T. Vetterling, and B. P. Flannery, *Numerical Recipes*, 2nd ed. (Cambridge University Press, Cambridge, 1992), p. 554.
[24] Although it does not significantly affect the results, in peforming the linear fits shown in Fig. 7(b) we have allowed for the possibility of a constant term. The reason for this is that a constant background could arise because step-step repulsions restrict the amplitude of long-wavelength fluctuations. Constraining a single step to wander in a parabolic potential of strength per unit length cx^2 causes Eq. (2.4) to be modified to $1/A(q)L=(c+\tilde{\beta}/2)/kT$. If the value of c is taken to be λ_σ/l^2 as in Sec. VIII, then for $l=200$ nm and $1/A(q=0)L\approx 10^{-5}$ nm^{-3}, consistent with Fig. 7(b).
[25] R. M. Tromp and M.C. Reuter, Phys. Rev. Lett. **68**, 820 (1992).
[26] J. Tersoff and E. Pehlke, Phys. Rev. Lett. **68**, 816 (1992).
[27] B. Houchmandzadeh and C. Misbah, J. Phys. (France) I **5**, 685 (1995).
[28] If attachment and detachment occurred only in units of pairs of dimers at these temperatures, then ω should be taken as the area of a pair of dimers, and τ_a would then be the time between attachments of dimer pairs.
[29] O. L. Alerhand, D. Vanderbilt, R. D. Meade, and J. D. Joannopoulos, Phys. Rev. Lett. **61**, 1973 (1988).
[30] A. García and J. E. Northrup, Phys. Rev. B **48**, 17 350 (1993).
[31] The purpose of this assumption is to simplify the algebra: when the potential is quadratic, the Langevin equation (Ref. 8) is linear — so each Fourier component, including the infinite-wavelength component of the step edge, fluctuates independently of all the others (as it does when the fluctuations are only limited by step-edge tension). This approximation is clearly going to be worse when the step edges come close to each other.